Libby WF, Anderson EC and Arnold JR (1949) Age determination by radiocarbon content: world-wide assay of natural radiocarbon. *Science* 109: 227–228.

Measures CI and Edmond JM (1982) Beryllium in the water column of the Central Pacific. *Nature* 297: 51–53.

Murray JW, Barber RT, Roman MR, Bacon MP and Feely RA (1994) Physical and biological controls on carbon cycling in the equatorial Pacific. *Science* 266: 58–65.

Raisbeck GM and Yiou F (1999) ^{129}I in the oceans: origins and applications. *Science of the Total Environment* 237/238: 31–41.

Schlosser P and Smethie Jr WM (1995) Transient tracers as a tool to study variability of ocean circulation. In: *Natural Climate Variability on Decade-to-century Time Scales,* pp. 274–289. Washington: National Research Council.

COUPLED SEA ICE–OCEAN MODELS

A. Beckmann and G. Birnbaum, Alfred-Wegener-Institut für Polar und Meeresforschung, Bremerhaven, Germany

doi:10.1006/rwos.2001.0473

Introduction

Oceans and marginal seas in high latitudes are seasonally or permanently covered by sea ice. The understanding of its growth, movement, and decay is of utmost importance scientifically and logistically, because it affects the physical conditions for air–sea interaction, the large-scale circulation of atmosphere and oceans and ultimately the global climate (e.g., the deep and bottom water formation) as well as human activities in these areas (e.g., ship traffic, offshore technology).

Coupled sea ice–ocean models have become valuable tools in the study of individual processes and the consequences of ice–ocean interaction on regional to global scales. The sea ice component predicts the temporal evolution of the ice cover, thus interactively providing the boundary conditions for the ocean circulation model which computes the resulting water mass distribution and circulation.

A number of important feedback processes between the components of the coupled system can be identified which need to be adequately represented (either resolved or parameterized) in coupled sea ice–ocean models (see **Figure 1**):

- ice growth through freezing of sea water, the related brine release and water mass modification;
- polynya maintenance by continuous oceanic upwelling;
- lead generation by lateral surface current shear and divergence;
- surface buoyancy loss causing oceanic convection; and
- pycnocline stabilization in melting regions.

Not all of these are equally important everywhere, and it is not surprising that numerous variants of coupled sea ice–ocean models exist, which differ in physical detail, parameterizational sophistication, and numerical formulation. Models for studies with higher resolution usually require a higher level of complexity.

The main regions for applying coupled sea ice–ocean models are the Arctic Ocean, the waters surrounding Antarctica, and marginal seas of the Northern Hemisphere (e.g., Baltic Sea, Hudson Bay). A universally applicable model needs to include (either explicitly or by adequate parameterization) the specific mechanisms of each region, e.g., mainly seasonal variations of the ice cover or the presence of thick, ridged multiyear ice.

This article describes the philosophy and design of large- and mesoscale prognostic dynamic–thermodynamic sea ice models which are coupled to primitive equation ocean circulation models (*see* **General Circulation Models**). The conservation principles, the most widely used parameterizations, several numerical and coupling aspects, and model evaluation issues are addressed.

Basics

Sea water and sea ice as geophysical media are quite different; whereas the liquid phase is continuous, three-dimensional, and largely incompressible, the solid phase can be best characterized as granular, two-dimensional and compressible. Both share a high degree of nonlinearity, and many direct feedbacks between oceanic and sea ice processes exist.

Today's coupled sea ice–ocean models are Eulerian; granular Lagrangian models, which consider the floe–floe interaction explicitly, exist but have so far not been fully coupled to ocean circulation models. Originally designed for use with large-scale coarse resolution ocean models, sea ice in state-of-the-art models is treated as a continuous medium. Following the continuum hypothesis only the average effect

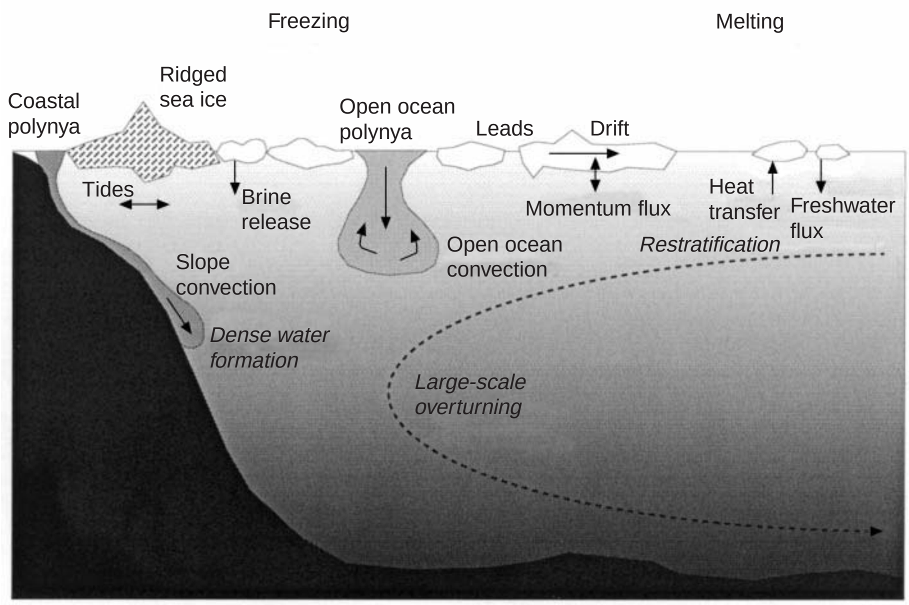

Figure 1 Cartoon of coupled sea ice–ocean processes. Effects in the ocean are in *italics*.

of a large number of ice floes is considered, assuming that averaged ice volume and velocities are continuous and differentiable functions of space and time.

Thus, very similar numerical methods are being applied to both sea water and sea ice, which greatly facilitates the coupling of models of these two components of the climate system. Conceptually, the continuum approach limits the applicability of sea ice models to grid spacings that are much larger than typical floes, i.e., several to several tens of kilometers. Typical values are 100–300 km for global climate studies, 10–100 km for regional climate simulations and about 2 km for process studies and quasi-operational forecasts. The latter cases are stretching the continuum concept for sea ice quite a bit, but still give reasonable results.

State-of-the-art coupled sea ice–ocean models are based on two principles for the description of sea ice, the conservation of mass and momentum, covering its thermodynamics and dynamics. Mass conservation for snow is also taken into account. A snow layer modifies the thermal properties of the ice cover through an increased albedo and reduced conductivity. This leads to delayed surface melting and lower basal freezing rates. In the following description sea ice is frozen sea water, and ice is the sum of sea ice and snow.

The temporal change of sea ice and snow volume due to local sources/sinks and drift is described by the mass conservation equation

$$\frac{\partial h_{(i,s)}}{\partial t} + \nabla \cdot (\vec{v}_i h_{(i,s)}) = S^{thdyn}_{h_{(i,s)}} \qquad [1]$$

where $h_{(i,s)}$ is the sea ice and snow volume per unit area (with $h = h_i + h_s$), respectively, $\vec{v}_i$ is the two-dimensional ice velocity vector and $S^{thdyn}_{h_{(i,s)}}$ denotes the thermodynamic sources and sinks for sea ice and snow. The corresponding ice velocities are obtained from the momentum equation

$$(\rho_i h_i + \rho_s h_s)\left[\frac{\partial \vec{v}_i}{\partial t} + \vec{v}_i \cdot \nabla \vec{v}_i + f\vec{k} \times \vec{v}_i + g\nabla \mathscr{H}\right] = \vec{\tau}_{ai} - \vec{\tau}_{iw} + \vec{\mathscr{F}}_i \qquad [2]$$

where the local time rate of change, advection of momentum and the accelerations due to Coriolis are included. The wind stress $\vec{\tau}_{ai}$ is external to the coupled sea ice–ocean model; the ocean surface current stress $\vec{\tau}_{iw}$ and the sea surface height $\mathscr{H}$ is part of the coupling to the ocean. The so-called ice stress term $\vec{\mathscr{F}}_i$ summarizes all internal forces generated by floe–floe interactions.

Subgridscale Parameterizations

The granular nature of the medium, combined with the strong sensitivity of both thermodynamics and dynamics on the number, size, and thickness of individual ice floes requires the inclusion of a subgridscale structure of the modeled ice.

Ice Classes

An obvious assumption is that of a subgridscale ice thickness distribution. In this widely used approach the predicted ice volume h is thought to be the average of several compartments, the thermodynamic ice classes, which represent both thinner and thicker ice and possibly include open water. The relative contribution of an ice class is fixed (e.g., uniform between 0 and twice the average ice thickness). For each ice class, a separate thermodynamic balance is computed; the resulting fluxes are then averaged according to their relative areal coverage.

Ice Categories

As the subgridscale distribution of ice thickness will change with time and location, an even more sophisticated approach considers time-evolution of the volume of each compartment, which is then called an ice category. The form of these prognostic equations follows the conservation eqn [1]. Different subgridscale ice velocities are not taken into account; the advection of all compartments takes place with the resolved velocity field.

Models with several ice categories are in use. A minimum requirement, however, has been identified in the discrimination between ice-covered areas and open water. Then the prognostic equation for ice volume [1] is accompanied by a formally similar equation for ice concentration, i.e., the percentage of ice-covered area per unit area A,

$$\frac{\partial A}{\partial t} + \nabla \cdot (\vec{v}_i A) = S_A^{thdyn} + S_A^{thdyn} \qquad [3]$$

Thermodynamic sources and sinks S_A^{thdyn} for ice concentration are chosen empirically and involve parameterizations of subgridscale thermodynamic melting and freezing. The conceptual *ansatz*:

$$S_A^{thdyn} = \frac{1-A}{h_{cls}} \max\left[0, \frac{\partial h}{\partial t}\right] + \frac{A}{h_{opn}} \min\left[\frac{\partial h}{\partial t}, 0\right] \qquad [4]$$

describes the formation of new ice between the ice floes with the first term on the right hand side; here h_{cls} is the so-called lead closing parameter. The second term parameterizes basal melting of sea ice with a similar approach involving h_{opn}. The coefficients are often derived from the assumed internal structure of the ice-covered portion of the grid cell, the ice classes. The dynamic source/sink term S_A^{dyn} follows from the constitutive law (see section on dynamics below). Conceptually, the ice concentration (or compactness) A has to lie between 0 and 1, which has to be enforced separately.

With the introduction of an ice concentration, the ice volume h has to be replaced by the actual ice thickness

$$h^* = \frac{h}{A} \qquad [5]$$

i.e., the mean value of individual floe height, such that the total ice volume per grid box is not affected by this approach.

An approach using two categories, open water and ice-covered areas with an internal structure (ice classes), has been proven highly adequate for a large number of situations.

Thermodynamics

Mass conservation for ice is closely tied to the heat balance at its surfaces. Sea ice forms, if the freezing temperature of sea water is reached. The surface freezing point T_f (in K) is a function of salinity, estimated by the polynomial approximation

$$T_f = 273.15 - 0.0575 S_w + 1.710523 \times 10^{-3} S_w^{3/2} - 2.154996 \times 10^{-4} S_w^2 \qquad [6]$$

where S_w is the sea surface salinity.

The majority of today's sea ice thermodynamics models is based on a one-dimensional (vertical) heat diffusion equation, which for sea ice (without snow cover) reads

$$\rho_i c_{pi} \frac{\partial T_i}{\partial t} = \frac{\partial}{\partial z}\left(k_i \frac{\partial T_i}{\partial z}\right) + K_i I_{oi} \exp[-K_i z] \qquad [7]$$

Here, T_i, ρ_i, c_{pi} and k_i are the sea ice temperature, density, specific heat, and thermal conductivity, respectively. The net short-wave radiation at the sea ice surface is I_{oi} and K_i is the bulk extinction coefficient.

If a snow cover is present, the penetrating short wave radiation is neglected and a second prognostic equation for the snow is solved:

$$\rho_s c_{ps} \frac{\partial T_s}{\partial t} = \frac{\partial}{\partial z}\left(k_s \frac{\partial T_s}{\partial z}\right) \qquad [8]$$

At the snow–sea ice interface, the temperatures and fluxes have to match.

Assuming that ice exists, the local time rate of change of ice thickness due to freezing of sea water or melting of ice is the result of the energy fluxes at the surface and the base of the ice. At the surface, the ice temperature and thickness change is determined from the energy balance equation:

$$\begin{aligned} Q_{a(i,s)} &= (1-\alpha_{(i,s)})(1-I_{oi})\mathscr{R}_{SW}^{\downarrow} + \mathscr{R}_{LW}^{\downarrow} \\ &\quad - \varepsilon_{(i,s)}\sigma_o T_{0(i,s)}^4 + Q_l + Q_s + Q_c \\ &= \begin{cases} 0 & \text{if } T_{o(i,s)} < T_{m(i,s)} \\ -\rho_{(i,s)} L_{(i,s)} \frac{\partial h^*}{\partial t} & \text{if } T_{o(i,s)} = T_{m(i,s)} \end{cases} \end{aligned} \qquad [9]$$

where $T_{o(i,s)}$ and $T_{m(i,s)}$ are the surface and melting temperatures, respectively, $\rho_{(i,s)}$ and $L_{(i,s)}$ are the density and heat of fusion for sea ice and snow. Besides the conductive heat flux in the ice $Q_c = k_{(i,s)}\partial T_{(i,s)}/\partial t$ the following atmospheric fluxes are considered: downward short-wave radiation $\mathscr{R}^{\downarrow}_{\mathrm{SW}}(\phi, \lambda, A_{cl})$, net long-wave radiation $\mathscr{R}^{\downarrow}_{\mathrm{LW}}(T_a, A_{cl}) - \varepsilon_{(i,s)}\sigma_o T^4_{o(i,s)}$, as well as sensible $Q_s(\vec{v}_a, T_a, T_{o(i,s)})$ and latent $Q_l(\vec{v}_a, q_a, q_{o(i,s)})$ heat fluxes. The albedos $\alpha_{(i,s)}$ and emissivities $\in_{(i,s)}$ are dependent on the surface structure of the medium (sea ice, snow). The atmospheric forcing data are:

- near-surface wind velocity $\vec{v}_a$;
- near-surface atmospheric temperature T_a;
- near-surface atmospheric dew point temperature T_d, or specific humidity q_a;
- cloudiness A_{cl};
- precipitation P and evaporation E (needed for the sea ice and snow mass balance).

Note that the wind velocity is also needed for the atmospheric forcing in the momentum eqn [2].

At the base of the ice (the sea surface), an imbalance of the conductive heat flux in the sea ice (Q_c) and the turbulent heat flux from the ocean

$$Q_{sw} = \rho_w c_{pw} c_h u_\star (T_f - T_{ml}) \qquad [10]$$

leads to a change in ice thickness:

$$Q_{iw} = -Q_{ow} - Q_c = -\rho_i L_i \frac{\partial h_i^*}{\partial t} \qquad [11]$$

Here, T_{ml} is the ocean surface and mixed layer temperature, c_h is the heat transfer coefficient and $u_\star$ is the friction velocity. In general, the main sink for ice volume is basal melting due to above-freezing temperatures in the oceanic mixed layer. The source for snow is a positive rate of P–E, if the air temperature is below the freezing point of fresh water. The main source for sea ice is basal freezing. However, the formation of additional sea ice on the upper ice surface is possible through a process called flooding. This conversion of snow into sea ice takes place when the weight of the snow exceeds the buoyancy of the ice and sea water intrudes laterally.

Often, the vertical structure of temperature is approximated by simple zero-, one- or two-layer formulations, with the resulting internal temperature profile being piecewise linear. The most simple approach, the zero-layer model, eliminates the capacity of the ice to store heat. However, it has been used successfully in areas where sea ice is mostly seasonal and thus relatively thin (< 1 m).

The specifics of the brine-related processes in the sea ice are difficult to implement in models. As a consequence, sea ice models usually assume constant sea ice salinity S_i of about 5 PSU (practical salinity units) to calculate the heat of fusion and the vertical heat transfer coefficient. The errors arising from this assumption are largest during the early freezing processes, when salt concentrations are considerably higher.

The open water part of each grid cell, where the atmosphere is in direct contact with the ocean, is treated like any other air–sea interface. The thermodynamic eqns [9] and [11] are modified to the radiative and heat fluxes between ocean and atmosphere. In the case of heat loss resulting in an ocean temperature below the freezing point T_f, new ice is formed:

$$\begin{aligned} Q_{aw} &= (1-\alpha)(1-I_{ow})\mathscr{R}^{\downarrow}_{\mathrm{SW}} + \mathscr{R}^{\downarrow}_{\mathrm{LW}} - \varepsilon_w \sigma_o T^4_{ow} \\ &\quad + Q_l + Q_s + Q_{sw} \\ &= \begin{cases} 0 & \text{if } T_{ow} > T_f \\ -\rho_i L_i \frac{\partial h_i^*}{\partial t} & \text{if } T_{ow} = T_f \end{cases} \end{aligned} \qquad [12]$$

In the case of above-freezing ocean surface temperatures, Q_{sw} follows from eqn [10] with T_f replaced by T_{ow}. An illustration summarizing the fluxes is given in **Figure 2**.

The solution of eqns [7], [8], [9] and [11] is conceptually straightforward but algebraically complicated in that it involves iterative solution of the energy balance equation to obtain the surface temperature.

Dynamics

Driven by wind and surface ocean currents, sea ice grown locally is advected horizontally. Free drift (the absence of internal ice stresses) is a good approximation for individual ice floes. In a compact ice cover, however, internal stresses will resist further compression and react to shearing stresses. These internal ice forces are expressed as the divergence of the isotropic two-dimensional internal stress tensor

$$\vec{\mathscr{F}}_i = \nabla \cdot \sigma \qquad [13]$$

which depends on the stress–strain relationship, where the deformation rates are proportional to the spatial derivatives of ice velocities. A general form of the constitutive law is

$$\sigma = \begin{pmatrix} \eta^{\left(\frac{\partial u_i}{\partial x} - \frac{\partial v_i}{\partial y}\right)} + \zeta\left(\frac{\partial u_i}{\partial x} + \frac{\partial v_i}{\partial y}\right) - \frac{1}{2}P_i & \eta^{\left(\frac{\partial u_i}{\partial y} + \frac{\partial v_i}{\partial x}\right)} \\ \eta^{\left(\frac{\partial u_i}{\partial y} - \frac{\partial v_i}{\partial x}\right)} & \eta^{\left(\frac{\partial v_i}{\partial y} - \frac{\partial u_i}{\partial x}\right)} + \zeta^{\left(\frac{\partial u_i}{\partial x} + \frac{\partial v_i}{\partial y}\right)} - \frac{1}{2}P_i \end{pmatrix} \quad [14]$$

here, ζ and η are nonlinear viscosities for compression and shear. P_i is the ice strength.

The most widely used sea ice rheology is based on the viscous–plastic approach. Introduced as the result of the ice dynamics experiment AIDJEX, it has proven to be a universally applicable rheology. It treats the ice as a linear viscous fluid for small deformation rates and as a rigid plastic medium for

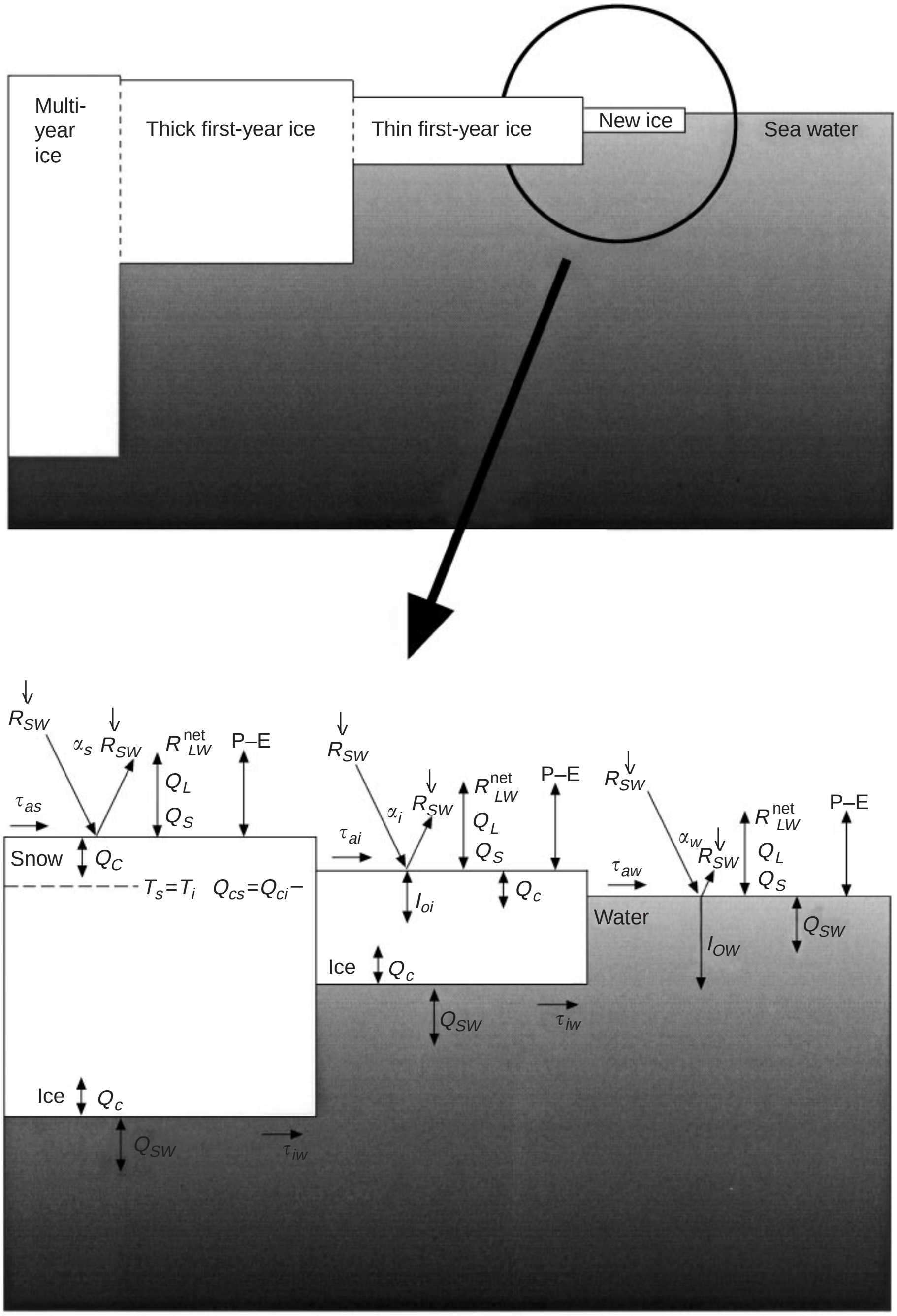

Figure 2 Schematic of the concept of ice classes/categories, surface energy balance and the ice–ocean flux coupling. The upper panel shows a grid cell covered with several classes/categories of ice, including open water. The lower panel is a detailed view at the fluxes between atmosphere, ice, and ocean, in the three cases: snow-covered sea ice, pure sea ice, and open water.

larger deformation rates. Simpler rheologies have been tested but could not reproduce the observed ice distributions and thicknesses nearly as well as the viscous–plastic approach. The viscosities are then

$$\zeta = e^2\eta = \frac{P_i}{2\Delta} \qquad [15]$$

where an elliptic yield curve of ellipticity e is assumed, with the deformation rate given by

$$\Delta = \left[\left\{\left(\frac{\partial u_i}{\partial x}\right)^2 + \left(\frac{\partial v_i}{\partial y}\right)^2\right\}(1+e^{-2}) + \left(\frac{\partial u_i}{\partial y} + \frac{\partial v_i}{\partial x}\right)^2 e^{-2} + 2\frac{\partial u_i}{\partial x}\frac{\partial v_i}{\partial y}(1-e^{-2})\right]^{1/2} \qquad [16]$$

In particular, internal forces are only important for densely packed ice floe fields, i.e., for ice concentrations exceeding 0.8. Most sea ice models take this into account by assuming that the ice strength is

$$P_i = P^* h \exp[-C^*(1-A)] \qquad [17]$$

where P^* and C^* are empirical parameters. The same functional dependence is also used successfully to describe the generation of open water areas through shear deformation, which is parameterized by

$$S_A^{dyn} = -0.5(\Delta - |\nabla \cdot \vec{v}_i|)\exp[-C^*(1-A)] \qquad [18]$$

Subgridscale processes like ridging and rafting can be successfully parameterized this way.

Coupling

Numerical ocean circulation models are described in **General Circulation Models**. A schematic illustration of the interactions in a coupled sea ice–ocean model is given in **Figure 3**. The coupling between the sea ice and ocean components is done via fluxes of heat, salt, and momentum. They enter the ocean model through the surface boundary conditions to the vertically diffusive/viscous terms. Given the relative (to the depth of the ocean) small draught of the ice, it is assumed not to deform the sea surface, all boundary conditions are applied at the air–sea interface.

Due to the presence of subgridscale ice categories, the fluxes have to be weighed with the areal coverage of open water, and ice of different thickness. The resulting boundary conditions for the simplest two-category (ice and open water) case are:

$$A_v^M \frac{\partial \vec{v}_w}{\partial z}\bigg|_{z=0} = A\vec{\tau}_{iw} + (1-A)\vec{\tau}_{aw} \qquad [19]$$

$$A_v^T \frac{\partial T_w}{\partial z}\bigg|_{z=0} = -\frac{1}{\rho_w c_p}(AQ_{iw} + (1-A)Q_{aw}) \qquad [20]$$

$$A_v^S \frac{\partial S_w}{\partial z}\bigg|_{z=0} = (S_w - S_i)\frac{\rho_i}{\rho_w}\frac{\partial h_i}{\partial t} + S_w \begin{cases} P-E & \text{if } h=0 \\ P-E & \text{if } h>0, T_a>0 \\ (1-A)(P-E) & \text{if } h>0, T_a<0 \\ \frac{\rho_s}{\rho_w}\frac{\partial h^s}{\partial t} & \text{if } h_s>0, T_a>0 \end{cases} \qquad [21]$$

where the freshwater flux is converted into a salt flux, and the momentum exchange is parameterized (like the atmospheric wind forcing $\vec{\tau}_{aw}$ and $\vec{\tau}_{ai}$) in the form of the usual quadratic drag law:

$$\vec{\tau}_{iw} = \rho_w C_w |\vec{v}_i - \vec{v}_w| [(\vec{v}_i - \vec{v}_w)\cos\theta_{iw} + \vec{k}\times(\vec{v}_i - \vec{v}_w)\sin\theta_{iw}] \qquad [22]$$

Here, C_w is the drag coefficient and θ_{iw} the rotation angle. The vertical viscosities and diffusivities (A_v^M, A_v^T, A_v^S) are ocean model parameters.

The sea surface height required to compute the ice momentum balance is either taken directly from the ocean model (for free sea surface models) or computed diagnostically from the upper ocean velocities using the geostrophic relationship.

The described coupling approach can be used between any sea ice and ocean model, irrespective of vertical resolution, or the use of a special surface mixed layer model. However, the results may suffer from a grid spacing that does not resolve the boundary layer sufficiently well.

A technical complication results from the different timescales in ocean and ice dynamics. With the implicit solution of the ice momentum equations, time steps of several hours are possible for the evolution of the ice. General ocean circulation models, on the other hand, require much smaller time steps, and an asynchronous time-stepping scheme may be most efficient. In that case, the fluxes to the ocean model remain constant over the long ice model step, whereas the velocities of the ocean model enter the fluxes only in a time-averaged form, mainly to avoid aliasing of inertial waves.

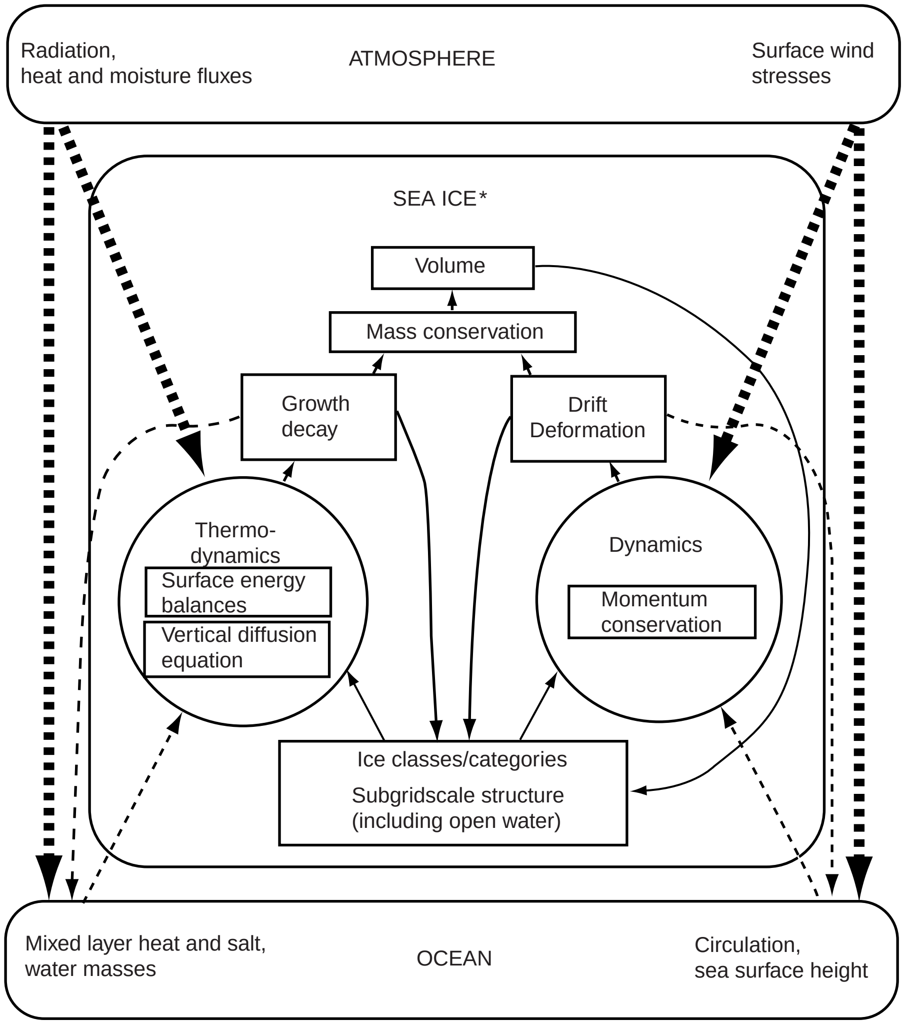

Figure 3 Concept of a coupled sea ice–ocean numerical model with prescribed atmospheric forcing. Thick broken arrows represent the atmospheric forcing, thin dashed arrows represent the coupling pathways between ice and ocean, and thin arrows indicate how the ice volume is computed from thermodynamical and dynamical principles (mass and momentum conservation), with the assumption of a subgridscale ice distribution. * Includes both sea ice and snow.

Numerical Aspects

Equations [1]–[3] are integrated as an initial boundary problem, usually on the same finite difference grid as the ocean model. A curvilinear coordinate system may be used to conform the ice model grid to an irregular coastline or to locally increase the resolution. The horizontal grid is usually staggered, either of the 'B' or 'C' type. Both have advantages and disadvantages: the 'B' grid has been favored because of the more convenient formulation of the stress terms and the better representation of the Coriolis term; the 'C' grid avoids averaging for the advection and pressure gradient terms. The treatment of coastal boundaries and the representation of flow through passages is also different.

Due to the large nonlinear viscosities in the viscous plastic approach, an explicit integration of the momentum equations would require time steps of the order of seconds, whereas the thickness equations can be integrated with time steps of the order of hours. Therefore, the momentum equations are usually solved implicitly. This leads to a nonlinear elliptic problem, which is solved iteratively. An explicit alternative has been developed for elastic–viscous–plastic rheology.

Other general requirements for numerical fluid dynamics models also apply: a positive definite and monotonic advection scheme is desired to avoid negative ice volume and concentration with the numerical implementation and algorithms depending on the computer architecture (serial, vector, parallel). Finally, the implementation needs to observe the singularities of the system of ice equations, which occur when h, A and Δ approach zero. Minimum values have to be specified to avoid vanishing ice volumes, concentrations, and deformation rates.

Model Evaluation

Modeling systems need to be validated against either analytical solutions or observational data. The various simplifications and parameterizations, as well as the specifics of the numerical implementation of both components' thermodynamics and dynamics and their interplay make this quite an extensive task. Analytical solutions of the fully coupled sea ice–ocean system are not known, and so model validation and optimization has to rely on geophysical observations.

Since *in situ* measurements in high latitude ice-covered regions are sparse, remote sensing products are being used increasingly to improve the spatial and temporal coverage of the observational database. Data sets of sea ice concentration, thickness and drift, ocean sea surface temperature, salinity, and height, are currently available, as well as hydrography and transport estimates.

Ice Variables

The most widely used validation variable for sea ice models is the ice concentration, i.e., the percentage of ice-covered area per unit area, which can be obtained from satellite observations. From these observations, maps of monthly mean sea ice extent are constructed, and compared to model output (see **Figure 4**). It should be noted though that the modeled ice concentrations represent a subgridscale parameterization with an empirically determined source/ sink relationship such that an optimization of a model with respect to this quantity may be misleading.

A more rigorous model evaluation focuses on sea ice thickness or drift, which is a conserved quantity and more representative of model performance. Unfortunately, 'ground truth' values of these variables are available in few locations and over relatively short periods only (e.g., upward looking sonar, ice buoys) and comparison of point measurements with

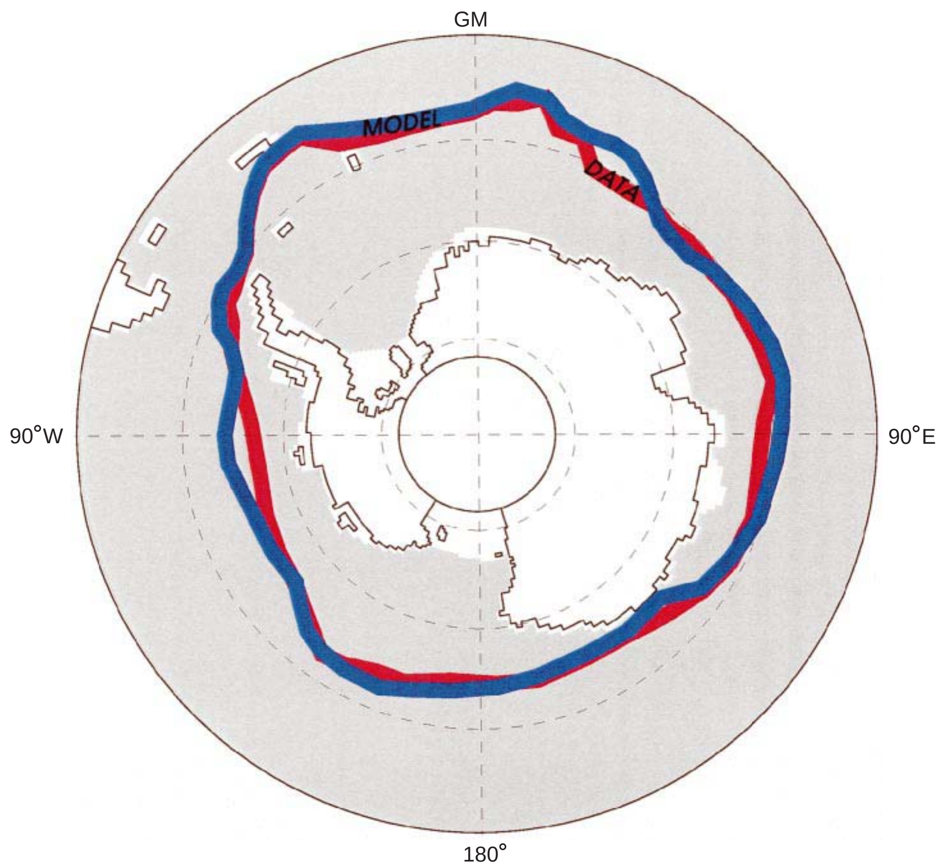

Figure 4 September 1987 simulated (blue) and remotely observed (red) sea ice edge around Antarctica. After Timmermann *et al.*, 2001.

coarse resolution model output is always problematic. A successful example is shown in **Figure 5**. The routine derivation of ice thickness estimates from satellite observations will be a major step in the validation attempts. The evaluation of ice motion is done through comparison between satellite-tracked and modeled ice buoys. Thickness and motion of first-year ice in free drift is usually represented well in the models, as long as atmospheric fields resolving synoptic weather systems are used to drive the system.

Ocean Variables

The success of the coupled system also depends on the representation of oceanic quantities. The model's temperature and salinity distribution as well as the corresponding circulation need to be consistent with prior knowledge from observations. The representation of water masses (characteristics, volumes, formation locations) can be validated against the existing hydrographic observational database, but a rigorous quantification of water mass formation products has been done only in few cases.

Parameter Sensitivities

Systematic evaluations of coupled model results have shown that a few parameter and conceptual choices are most crucial for model performance. For the sea ice component, these are the empirical source/sink terms for ice concentration, as well as the rheology. The most important oceanic processes are the vertical mixing (parameterizations), especially in the case of convection (*see* **Open Ocean Convection**). In general, the formulation of the heat transfer between the oceanic mixed layer and the ice is central to the coupled system.

Finally, the performance of a coupled sea ice–ocean model will depend on the quality of the atmospheric forcing data; products from the weather centers (European Centre for Medium Range Weather Forecasts, National Centers for Environmental Prediction/National Center for Atmospheric Research) provide consistent, but still rather coarsely resolved atmospheric fields, which have their lowest overall quality in high latitudes, especially in areas of highly irregular terrain and for the P–E and cloudiness fields. Some errors, even systematic ones, are presently unavoidable.

All these data products are available with different temporal resolution. Unlike for stand-alone ocean models, which can be successfully run with climatological monthly mean forcing data, winds, sampled daily or 6-hourly, have been found necessary to produce the observed amount of ridging and lead formation in sea ice models.

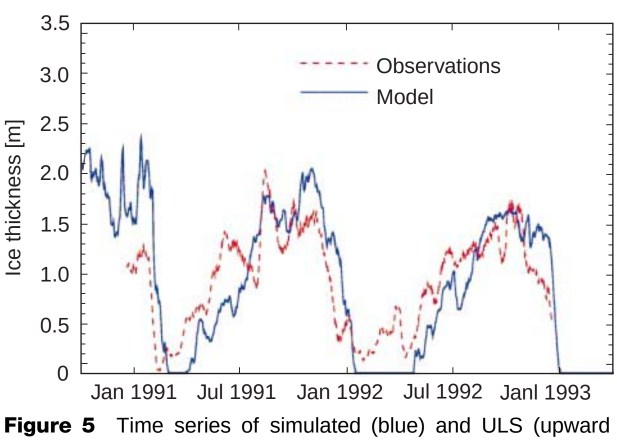

Figure 5 Time series of simulated (blue) and ULS (upward looking sonar) measured (red) sea ice thickness at 15°W, 70°S in the Weddell Sea. After Timmermann *et al.*, 2001

Conclusions

A large amount of empirical information is needed for coupled sea ice–ocean models and the often strong sensitivity to variations of these makes the optimization of such modeling systems a difficult task. Yet, several examples of successful simulation of fully coupled ice–ocean interaction exist, which qualitatively and quantitatively compare well with the available observations.

Coupled sea ice–ocean modeling is an evolving field, and much needs to be done to improve parameterizations of vertical (and lateral) fluxes at the ice–ocean interfaces. For climate studies, water mass variability on seasonal and interannual timescales needs to be captured by the model. For operational forecast purposes, the ice thickness distribution in itself is most important; here atmospheric data quality and assimilation methods become crucial. Obvious next steps may be the inclusion of tides, icebergs, and ice shelves.

Ultimately, however, a fully coupled atmosphere–ice–ocean model is required for the simulation of phenomena that depend on feedback between the three climate system components.

See also

Arctic Basin Circulation. Bottom Water Formation. Current Systems in the Southern Ocean. Forward Problem in Numerical Models. General Circulation Models. Ice–Ocean Interaction. Open Ocean Convection. Polynyas. Satellite Remote Sensing SAR. Sea Ice: Overview. Thermohaline Circulation. Under-ice Boundary Layer. Upper Ocean Heat and Freshwater Budgets. Upper Ocean Mixing Processes. Upper Ocean Mixing Processes. Weddell Sea Circulation.

Glossary of Symbols

c_h	heat transfer coefficient
$c_{p(i,s,w)}$	specific heat of sea ice/snow/water ($\mathrm{J\,kg^{-1}\,K^{-1}}$)
e	ellipticity
f	Coriolis parameter ($\mathrm{s^{-1}}$)
g	gravitational acceleration ($\mathrm{m\,s^{-2}}$)
h	ice (sea ice plus snow) volume per unit area (m)
$h_{(i,s)}$	sea ice/snow volume per unit area (m)
h^*	actual ice thickness (m)
$h^*_{(i,s)}$	actual sea ice/snow thickness (m)
h_{cls}, h_{opn}	lead closing/opening parameter (m)
$k_{(i,s)}$	thermal conductivity of sea ice/snow ($\mathrm{W\,m^{-1}\,K^{-1}}$)
$\vec{k}$	vertical unit vector
q_a	atmospheric specific humidity
$q_{o(i,s)}$	surface specific humidity of sea ice/snow
t	time (s)
$\vec{v}_i = (u_i, v_i)$	horizontal ice velocity ($\mathrm{m\,s^{-1}}$)
$u_\star$	friction velocity ($\mathrm{m\,s^{-1}}$)
$\vec{v}_a = (u_a, v_a)$	wind velocity ($\mathrm{m\,s^{-1}}$)
$\vec{v}_w = (u_w, v_w)$	ocean surface velocity ($\mathrm{m\,s^{-1}}$)
x, y, z	spatial directions (m)
A	ice concentration
A_{cl}	cloudiness
A_v^M, A_v^T, A_v^S	oceanic vertical mixing coefficients ($\mathrm{m^2\,s^{-1}}$)
C^*	empirical parameter
C_w	oceanic drag coefficient
$I_{o(i,w)}$	short wave radiation penetrating sea ice/water ($\mathrm{W\,m^{-2}}$)
E	evaporation ($\mathrm{m\,s^{-1}}$)
K_i	bulk extinction coefficient ($\mathrm{m^{-1}}$)
$L_{(i,s)}$	heat of fusion ($\mathrm{J\,kg^{-1}}$)
P	precipitation ($\mathrm{m\,s^{-1}}$)
P_i	ice strength ($\mathrm{N\,m^{-1}}$)
P^*	ice strength parameter ($\mathrm{N\,m^{-2}}$)
$Q_{a(i,s,w)}$	net energy flux between atmosphere and sea ice/snow/water ($\mathrm{W\,m^{-2}}$)
Q_c	conductive heat flux in the ice ($\mathrm{W\,m^{-2}}$)
Q_l, Q_s	atmospheric latent/sensible heat flux ($\mathrm{W\,m^{-2}}$)
Q_{iw}	turbulent heat flux at the ocean surface ($\mathrm{W\,m^{-2}}$)
Q_{sw}	oceanic sensible heat flux ($\mathrm{W\,m^{-2}}$)
$\mathcal{R}^{\downarrow}_{SW}, \mathcal{R}^{\downarrow}_{LW}$	downward short/long wave radiation ($\mathrm{W\,m^{-2}}$)
$S_{(i,w)}$	sea ice/sea water salinity (PSU)
T_a, T_i, T_w	air/ice/water temperature (K)
T_d	dew point temperature (K)
T_f	freezing temperature of sea water (K)
T_{ml}	oceanic mixed layer temperature (K)
$T_{m(i,s)}$	melting temperature of sea ice/snow at the surface (K)
$T_{o(i,s,w)}$	sea ice/snow/water surface temperature (K)
$\vec{\mathcal{F}}_i$	internal ice forces ($\mathrm{N\,m^{-2}}$)
$\mathcal{H}$	sea surface elevation (m)
$S_A^{(thdyn,\,dyn)}$	source/sink terms for ice concentration ($\mathrm{s^{-1}}$)
$S_{h(i,\,s)}^{thdyn}$	source/sink terms for sea ice/snow volume per unit area ($\mathrm{m\,s^{-1}}$)
$\alpha_{(i,\,s\,w)}$	sea ice/snow/sea water albedo
Δ	ice deformation rate ($\mathrm{s^{-1}}$)
$\varepsilon_{(i,\,s\,w)}$	sea ice/snow/sea water emissivity
η, ζ	nonlinear viscosities ($\mathrm{kg\,s^{-1}}$)
$\nabla = (\frac{\partial}{\partial x}, \frac{\partial}{\partial y})$	horizontal gradient operator
λ, ϕ	geographical longitude/latitude (deg)
$\rho_{(a,\,i,\,s,\,w)}$	densities of air/sea ice/snow/water ($\mathrm{kg\,m^{-3}}$)
σ	two-dimensional stress tensor ($\mathrm{N\,m^{-1}}$)
σ_o	Stefan-Boltzmann constant ($\mathrm{W\,m^{-2}\,K^{-4}}$)
θ_{iw}	turning angle (deg)
$\vec{\tau}_{ai}, \vec{\tau}_{iw}, \vec{\tau}_{aw}$	air-ice/ice-water/air-water stress ($\mathrm{N\,m^{-2}}$)

Appendix

A typical parameter set for simulations with coupled dynamic–thermodynamic ice–ocean models (e.g., Timmermann *et al.*, 2001), as shown in **Figures 4** and **5**, are

$\rho_a = 1.3\ \mathrm{kg\,m^{-3}}$
$\rho_i = 910\ \mathrm{kg\,m^{-3}}$
$\rho_s = 290\ \mathrm{kg\,m^{-3}}$
$\rho_w = 1027\ \mathrm{kg\,m^{-3}}$
e = 2
C* = 20
$\mathrm{P^*} = 2000\ \mathrm{N\,m^{-2}}$
$h_{cls} = 1$ m
$h_{opn} = 2\,\mathrm{h^*}$
$C_w = 3 \times 10^{-3}$
$c_h = 1.2 \times 10^{-3}$
$\alpha_w = 0.1$
$\alpha_i = 0.75$
$\alpha_i = 0.65$ (melting)
$\alpha_s = 0.8$
$\alpha_w = 0.7$ (melting)
$K_i = 0.04\ \mathrm{m^{-1}}$
$S_i = 5$ PSU
$\theta = 10$ degrees
$c_{pi} = 2000\ \mathrm{J\,K^{-1}\,kg^{-1}}$
$c_{pw} = 4000\ \mathrm{J\,K^{-1}\,kg^{-1}}$
$c_{pa} = 1004\ \mathrm{J\,K^{-1}\,kg^{-1}}$
$L_i = 3.34 \times 10^5\ \mathrm{J\,kg^{-1}}$
$L_s = 1.06 \times 10^5\ \mathrm{J\,kg^{-1}}$
$k_i = 2.1656\ \mathrm{W\,m^{-1}\,K^{-1}}$
$k_s = 0.31\ \mathrm{W\,m^{-1}\,K^{-1}}$

Further Reading

Curry JA and Webster PJ (1999) *Thermodynamics of Atmospheres and Oceans*, International Geophysics Series. London: Academic Press.
Fichefet T, Goosse H and Morales Maqueda M (1998) On the large-scale modeling of sea ice and sea ice–ocean interaction. In: Chassignet EP and Verron J (eds) *Ocean Modeling and Parameterization*, pp. 399–422. Dordrecht: Kluwer Academic.
Haidvogel DB and Beckmann A (1999) *Numerical Ocean Circulation Modeling*. London: Imperial College Press.
Hibler III WD (1979) A dynamic-thermodynamic sea ice model. *Journal of Physical Oceanography* 9: 815–846.
Kantha LH and Clayson CA (2000) *Numerical Models of Oceans and Oceanic Processes*. San Diego: Academic Press.
Leppäranta M (1998) The dynamics of sea ice. In: Leppäranta M (ed.) *Physics of Ice-Covered Seas* 1, 305–342.
Maykut GA and Untersteiner N (1971) Some results from a time-dependent thermodynamic model of sea ice. *Journal of Geophysical Research* 76: 1550–1575.
Mellor GL and Häkkinen S (1994) A review of coupled ice–ocean models. In: Johannessen OM, Muench RD and Overland JE (eds) *The Polar Oceans and Their Role in Shaping the Global Environment*. AGU Geophysical Monograph, 85, 21–31.
Parkinson CL and Washington WM (1979) A large-scale numerical model of sea ice. *Journal of Geophysical Research* 84: 311–337.
Timmermann R, Beckmann A and Hellmer HH (2001) Simulation of ice–ocean dynamics in the Weddell Sea. Part I: Model description and validation. *Journal of Geophysical Research* (in press).

CRUSTACEAN FISHERIES

J. W. Penn, N. Caputi and R. Melville-Smith, Fisheries WA Research Division, North Beach, WA, Australia

doi:10.1006/rwos.2001.0453

Introduction

The Crustacea are one of the most diverse groups of aquatic animals, occupying a wide variety of habitats from the shore to the deep ocean and the tropics to Arctic waters, and extending into fresh water and in some cases on to land for part of their life history.

Crustacean species contribute in the order of 7 million tonnes annually, or about 6–8% of the total world supply of fish, according to FAO statistics. Approximately 75% of this volume is from harvesting wild stocks, with the remainder from aquaculture, dominated by the tropical marine and freshwater shrimps, crayfish, and crab species. Owing to their high market value as a sought-after high-protein food, crustaceans make up a disproportionate share of the value of the world's seafoods. As a result of their high value, crustacean fisheries are generally heavily exploited and require active management to be sustained. Research to underpin management of these resources has been undertaken in many parts of the world, and particularly Australia where, unusually, lobsters and shrimps are the dominant fisheries.

Crustacean fisheries are focused on the more abundant species, particularly those in relatively shallow, accessible areas. Shrimps are the most important wild fishery products, followed by the crabs, lobsters, and krill.

Biology and Life History

Fisheries research on crustacean stocks is significantly influenced by their unusual life history and biology. A unique feature of crustaceans is that they all must undergo a regular process of molting (casting off their outer shell or exoskeleton) to grow. Once the old shell is cast off, the animal absorbs water to swell or 'grow' to a larger size before the shell hardens. Volume increase at a molt varies between species, but typically results in a gain in the range of 10–60%. The molt also serves as an opportunity to regenerate damaged limbs, such as legs or antennae, although regeneration results in lower or even negative growth increments. This molting process occurs throughout all stages of the life history and is often correlated with environmental factors such as temperature, moon phase, or tidal cycles. Because of this mechanism, growth occurs as a series of discrete 'steps' rather than a 'smooth' increase over time and is complicated to measure. Growth rates are highly dependent on water